Supporting Information

In-Situ Grown, Passivator-Modulated Anodization derived Synergistically Well Mixed Ni-Fe Oxides from Ni Foam as High Performance Oxygen Evolution Reaction Electrocatalyst

Xui-Fang Chuah, Cheng-Ting Hsieh, Chun-Lung Huang, Duraisamy Senthil Raja, Hao-Wei Lin, and Shih-Yuan Lu*

Department of Chemical Engineering, National Tsing Hua University, Hsinchu 30013, Taiwan, Republic of China.

*Corresponding author: sylu@mx.nthu.edu.tw

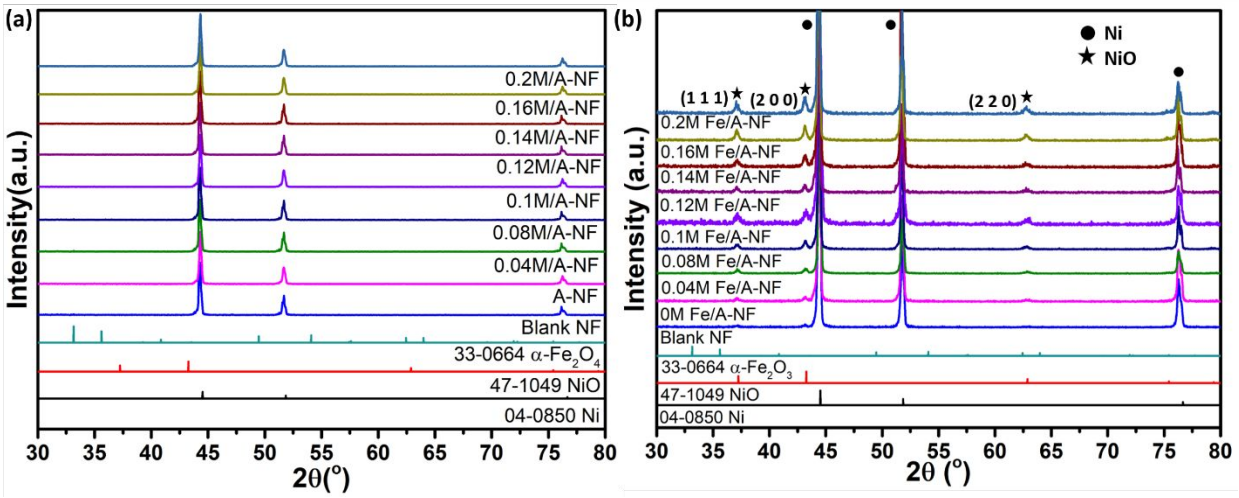

Fig. S1 (a) XRD patterns of anodized electrodes. (b) XRD patterns of anodized electrodes annealed under Argon atmosphere to confirm formation of oxide layer.

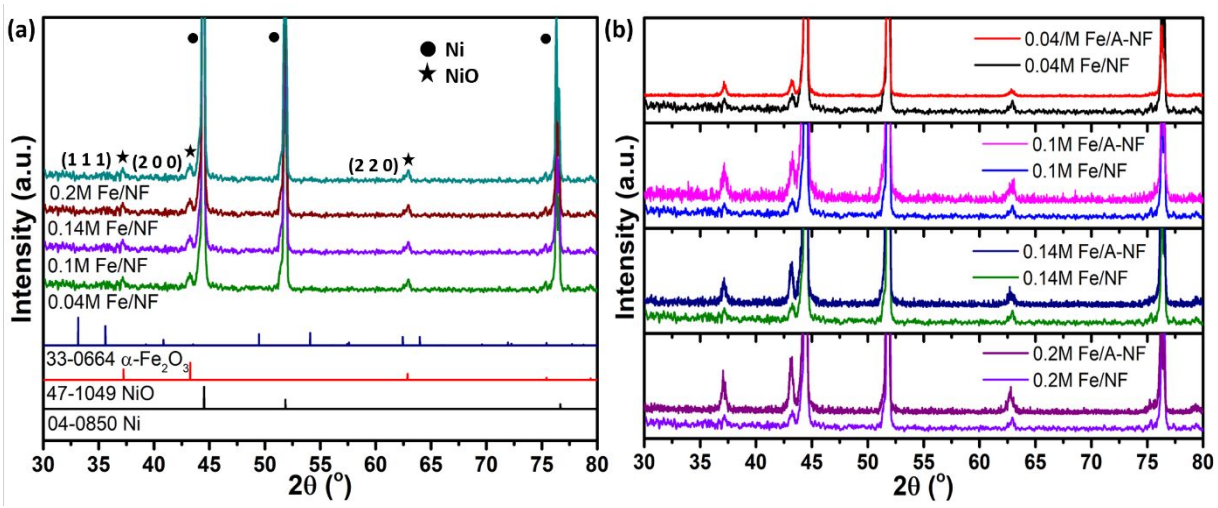

Fig. S2 (a) XRD patterns of annealed samples after anodization without NH_4F. (b) Comparison of annealed samples after anodization with (/A-NF series) and without (/NF series) NH_4F.

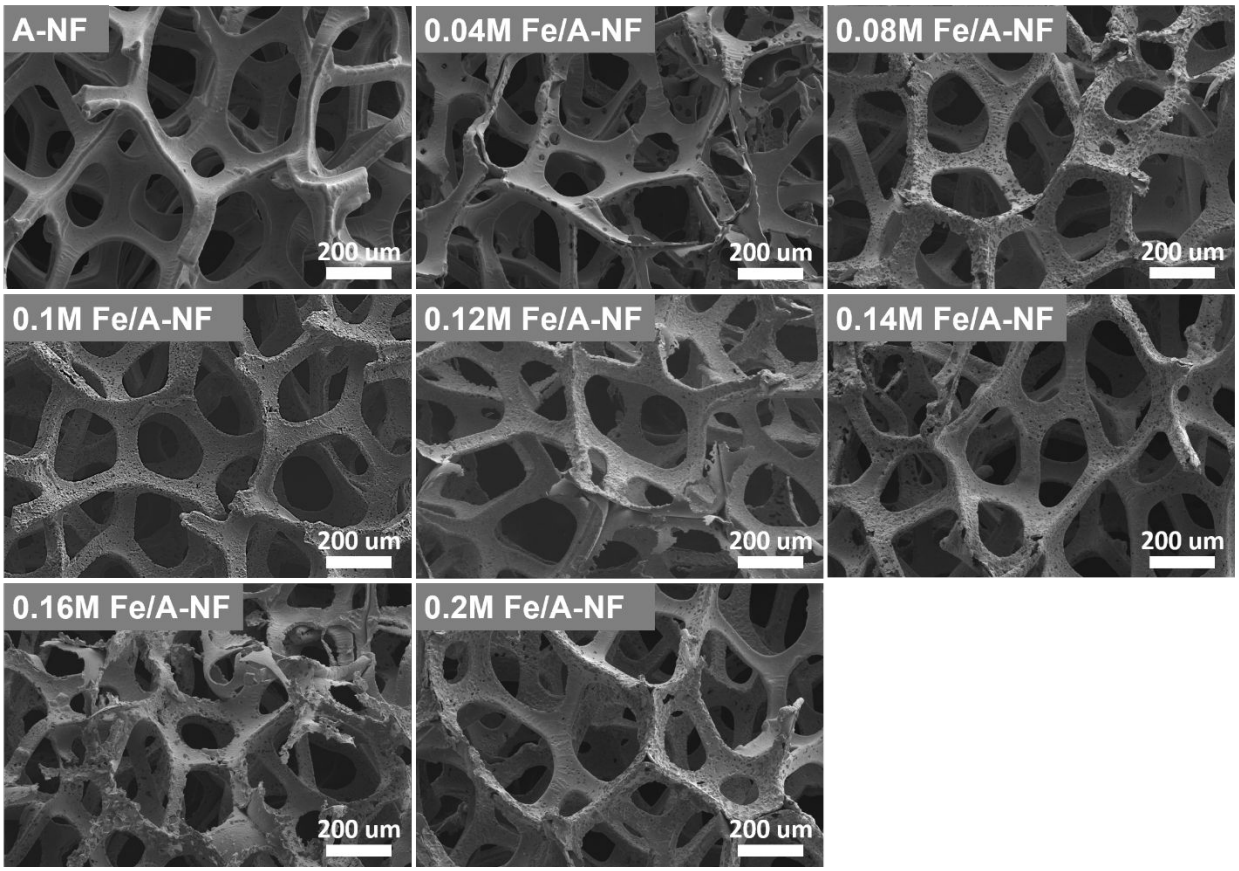

Fig. S3 SEM images of anodized samples at magnification of 100.

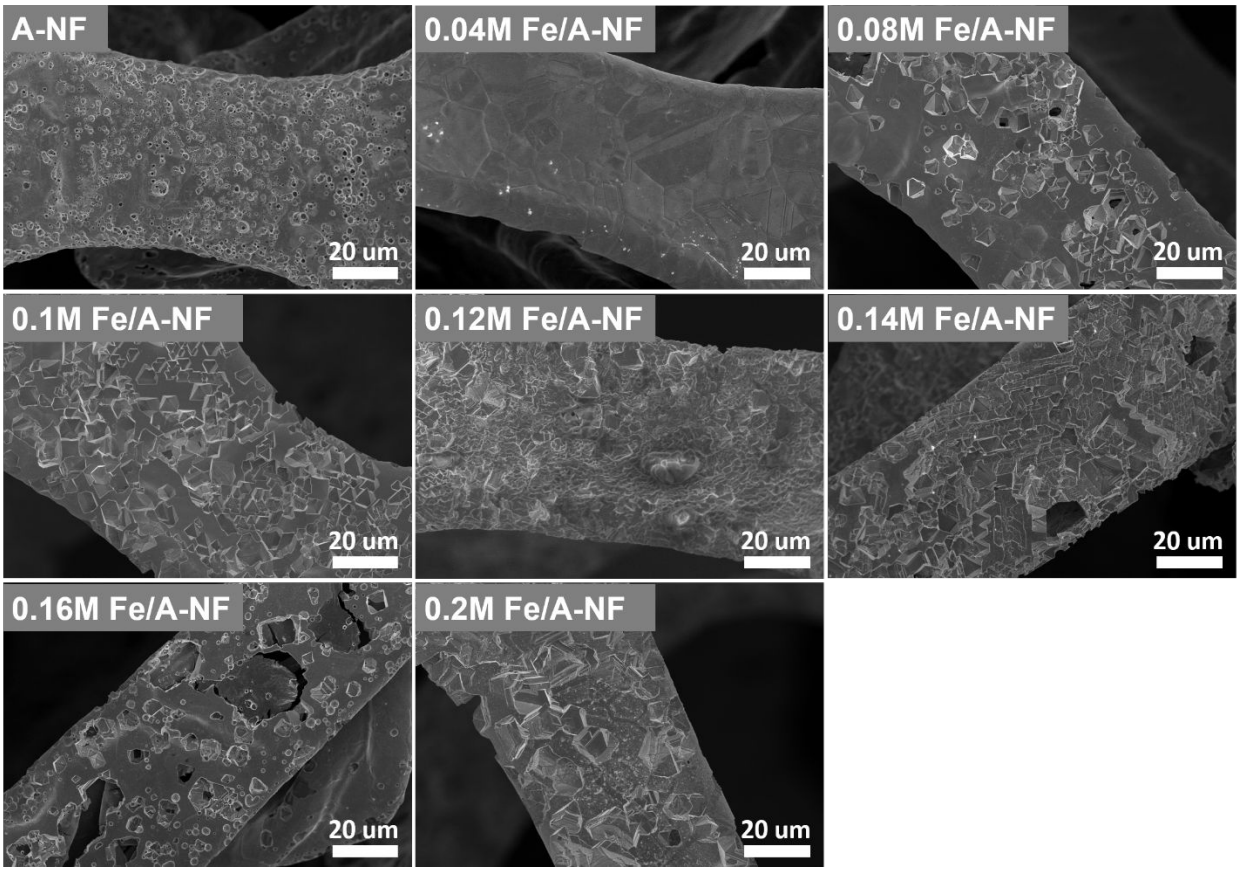

Fig. S4 SEM images of anodized samples at magnification of 1k.

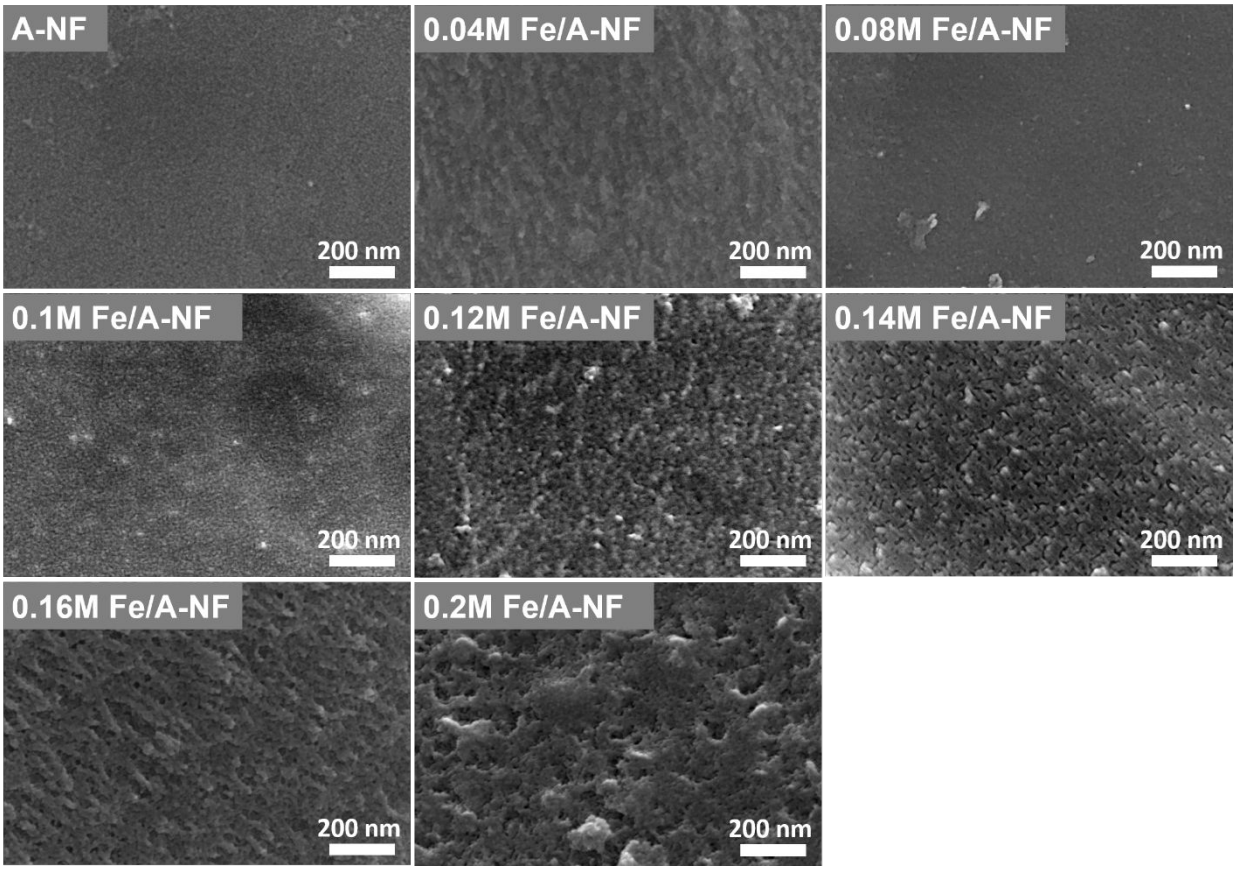

Fig. S5 SEM images of anodized samples at magnification of 100k.

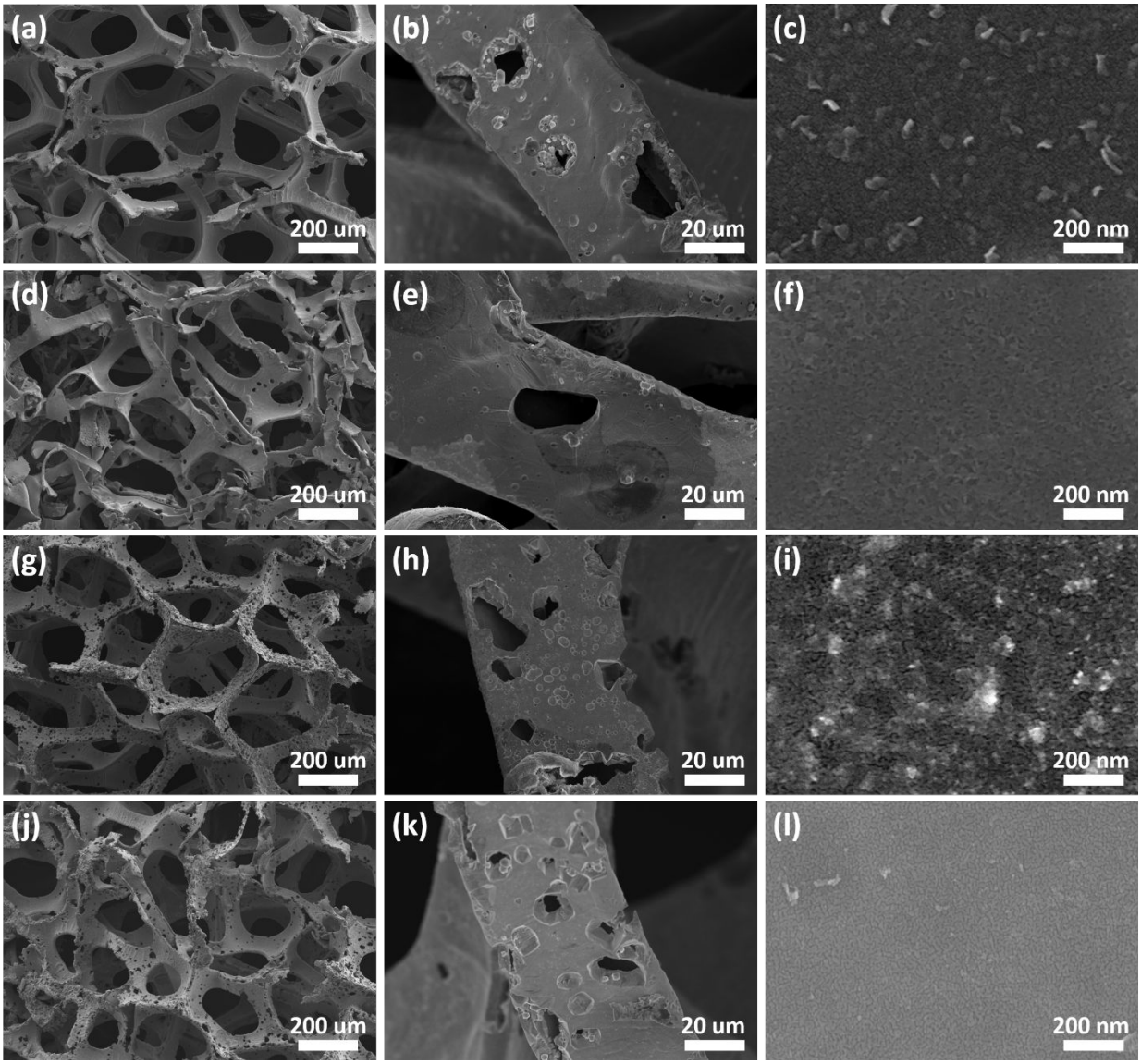

Fig. S6 SEM images of (a), (b), (c) 0.04M Fe/NF, (d), (e), (f) 0.1M Fe/NF, (g), (h), (i) 0.14M Fe/NF, and (j), (k), (l) 0.2M Fe/NF.

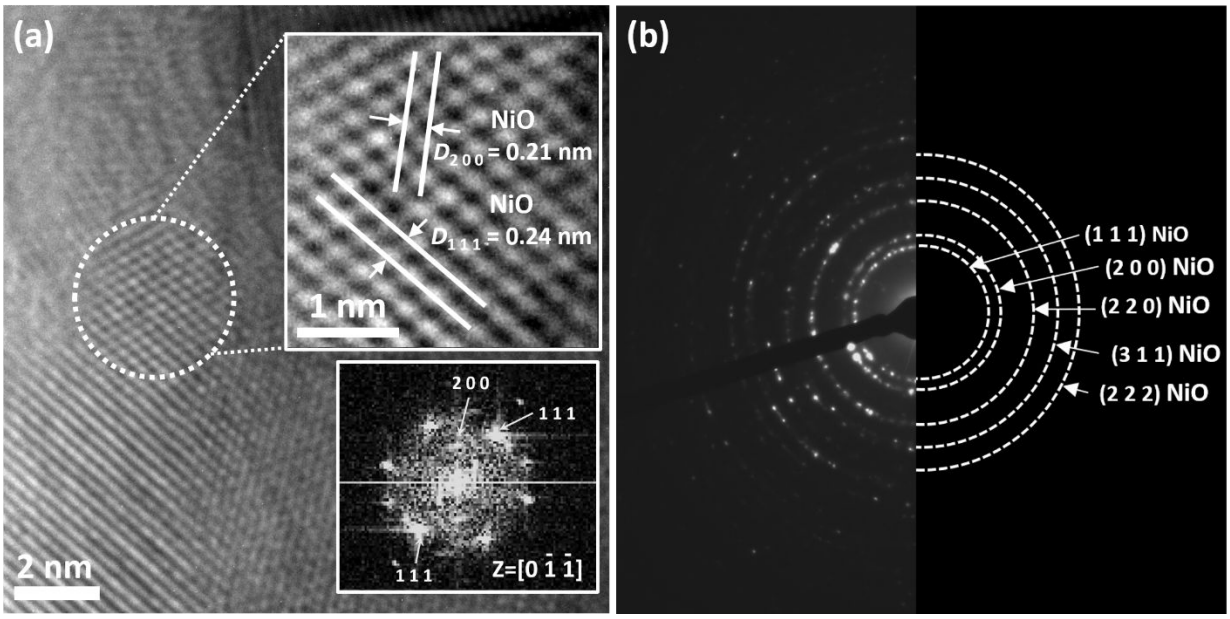

Fig. S7 (a) HRTEM image of A-NF, insets: locally enlarged HRTEM of white circled region and corresponding FFT pattern obtained from white circled region. (b) SAED patterns of A-NF.

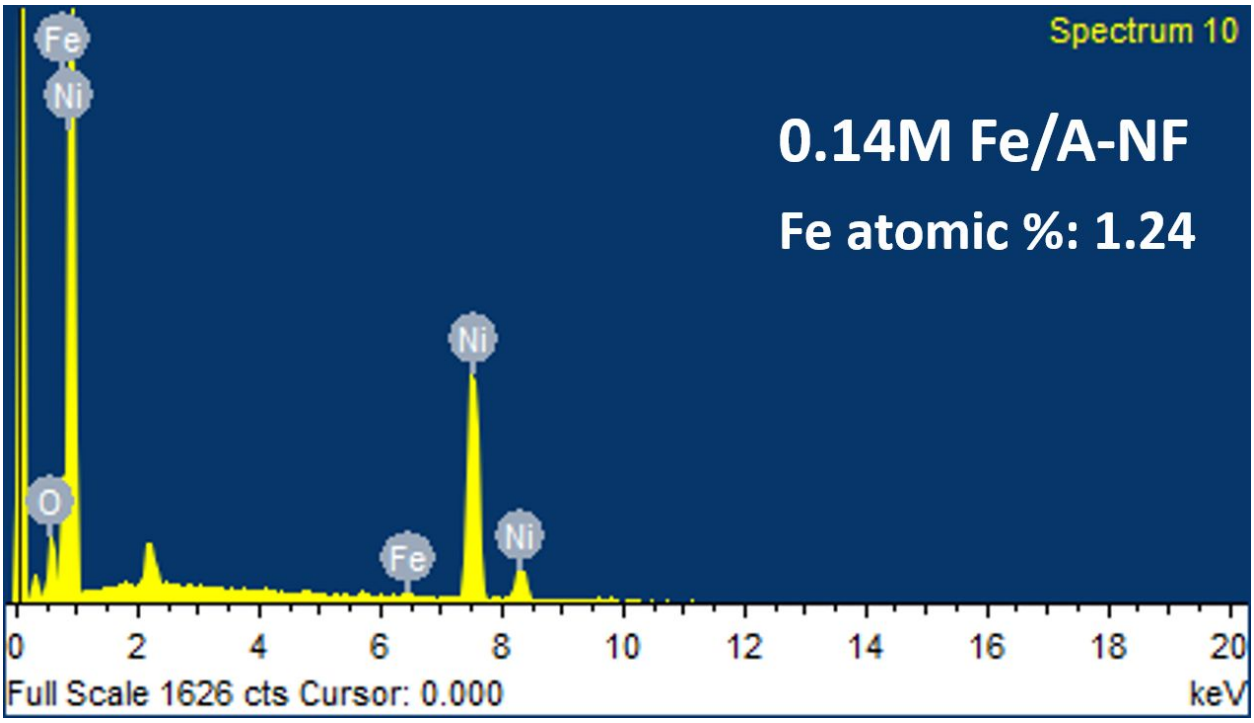

Fig. S8 EDX spectrum of sample 0.14M Fe/A-NF, confirming presence of Fe in sample.

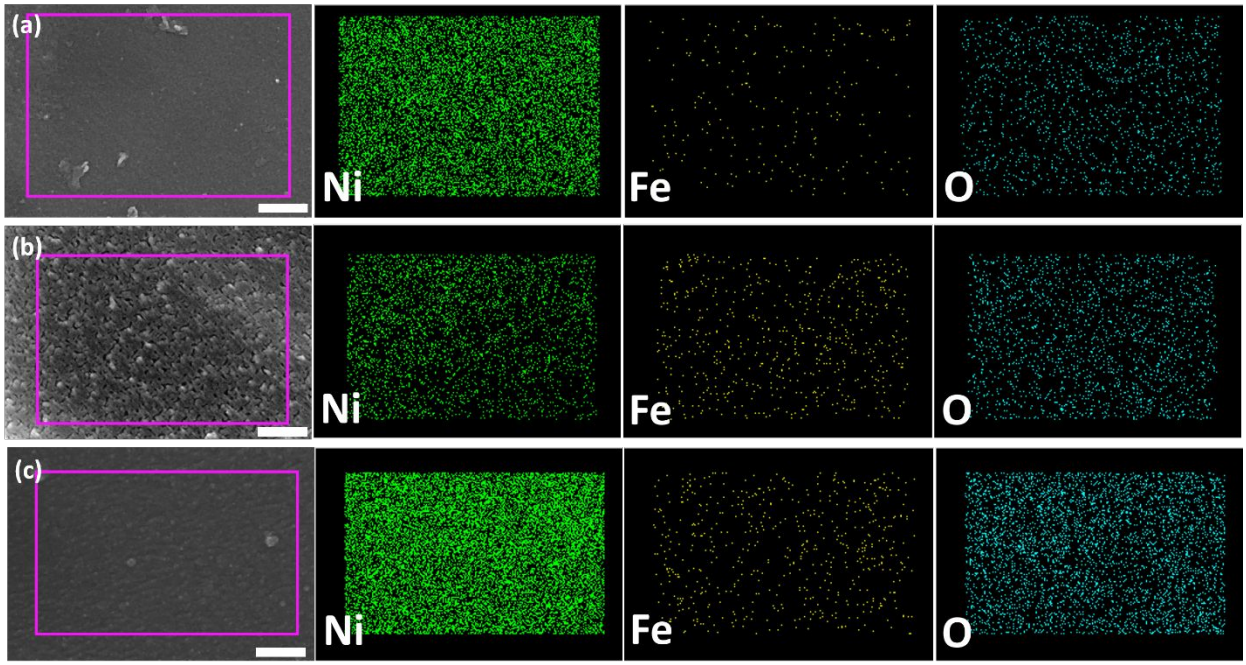

Fig. S9 Elemental mapping of samples: (a) 0.08M Fe/A-NF, (b) 0.14M Fe/A-NF, (c) 0.2M Fe/A-NF.

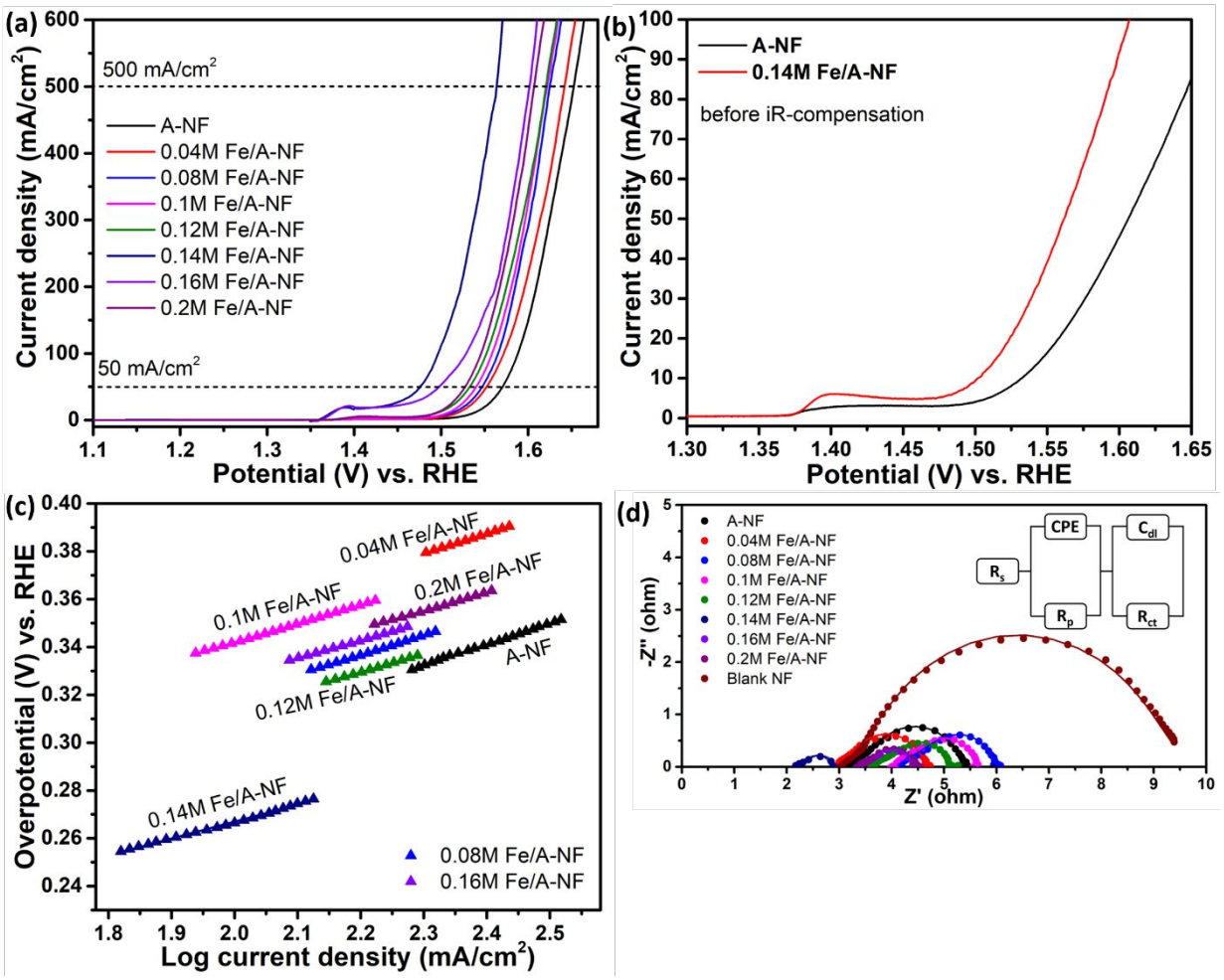

Fig. S10 OER activities of electrodes. (a) LSV polarization curves. (b) LSV polarization curves without iR-compensation. (c) Tafel slopes. (d) Nyquist plots recorded at 1.64 V vs. RHE, inset: equivalent circuit model.

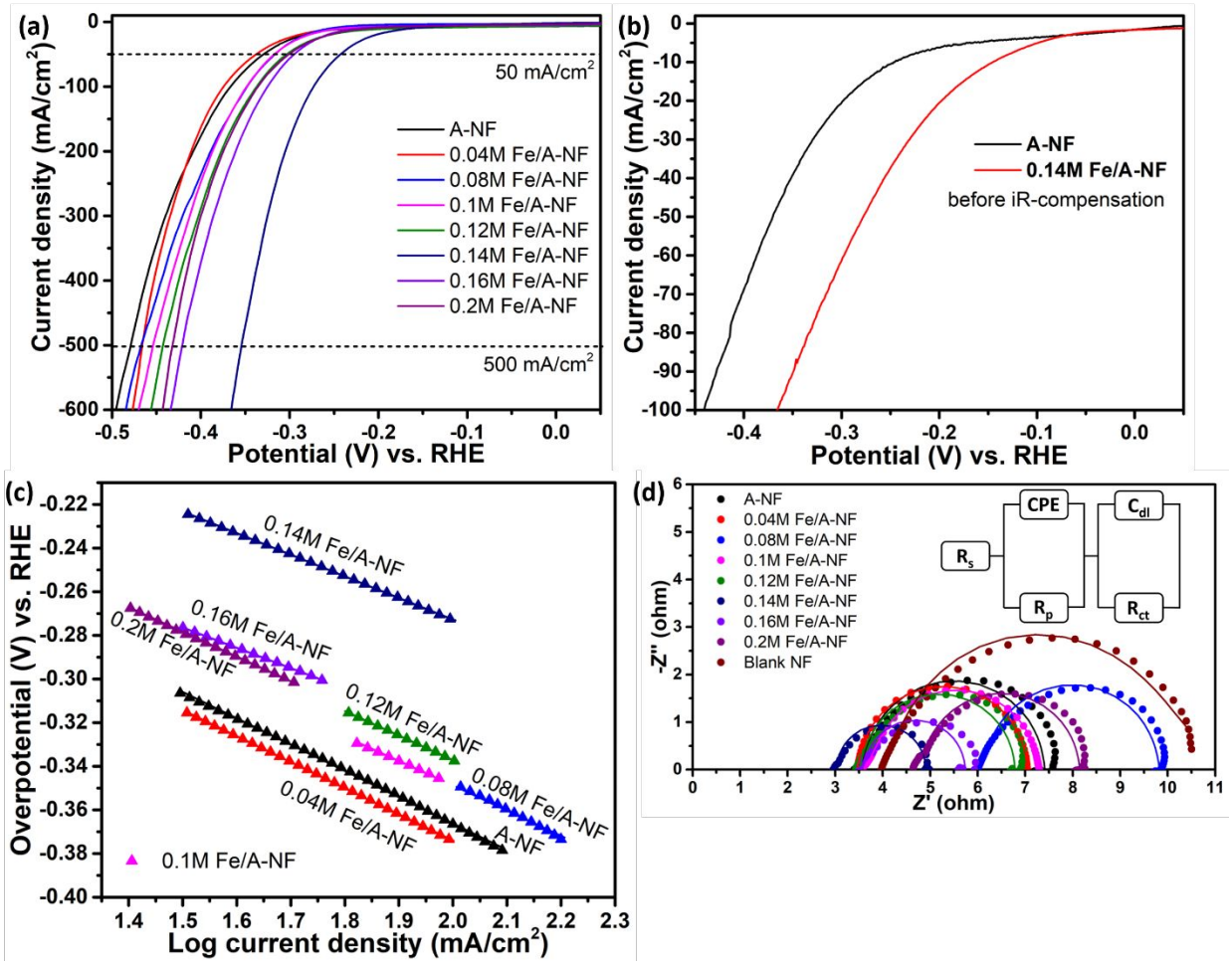

Fig. S11 HER activities of electrodes. (a) LSV polarization curves. (b) LSV polarization curves without iR-compensation. (c)Tafel slopes. (d) Nyquist plots recorded at -0.31 V vs. RHE, inset: equivalent circuit model.

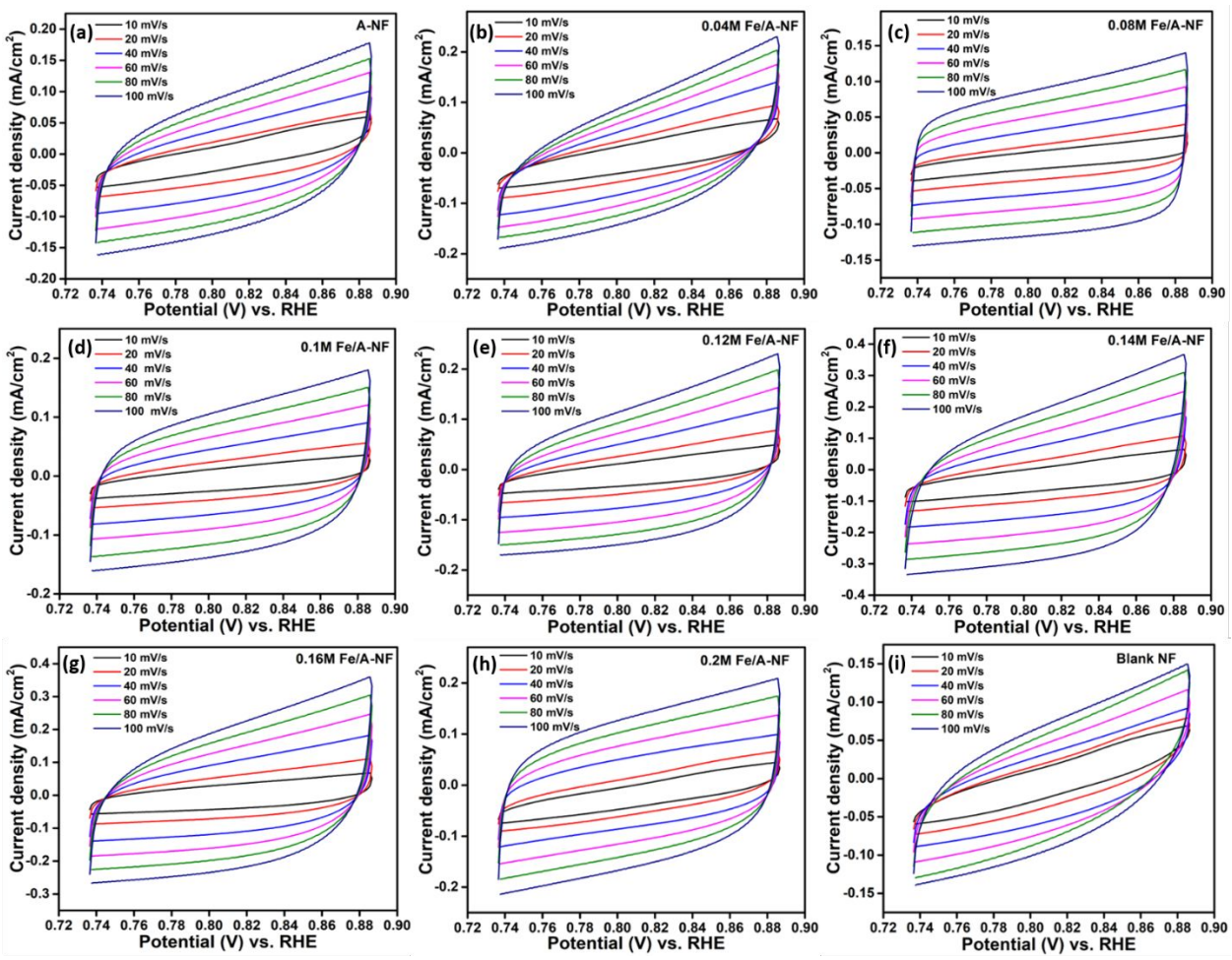

Fig. S12 Cyclic voltammograms recorded at increasing scan rates in 1M KOH of (a) A-NF, (b) 0.04M Fe/A-NF, (c) 0.08M Fe/A-NF, (d) 0.1M Fe/A-NF, (e) 0.12M Fe/A-NF, (f) 0.14M Fe/A-NF, (g) 0.16M Fe/A-NF, (h) 0.2M Fe/A-NF, (i) blank NF.

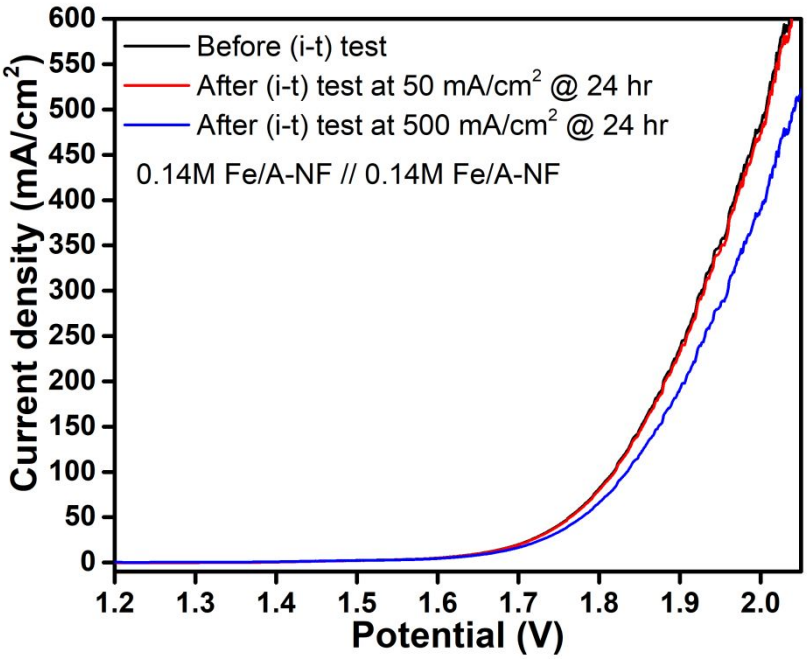

Fig. S13 LSV polarization curves of 0.14M Fe/A-NF//0.14M Fe/A-NF couple before and after chronoamperometric stability test for 24 hrs.

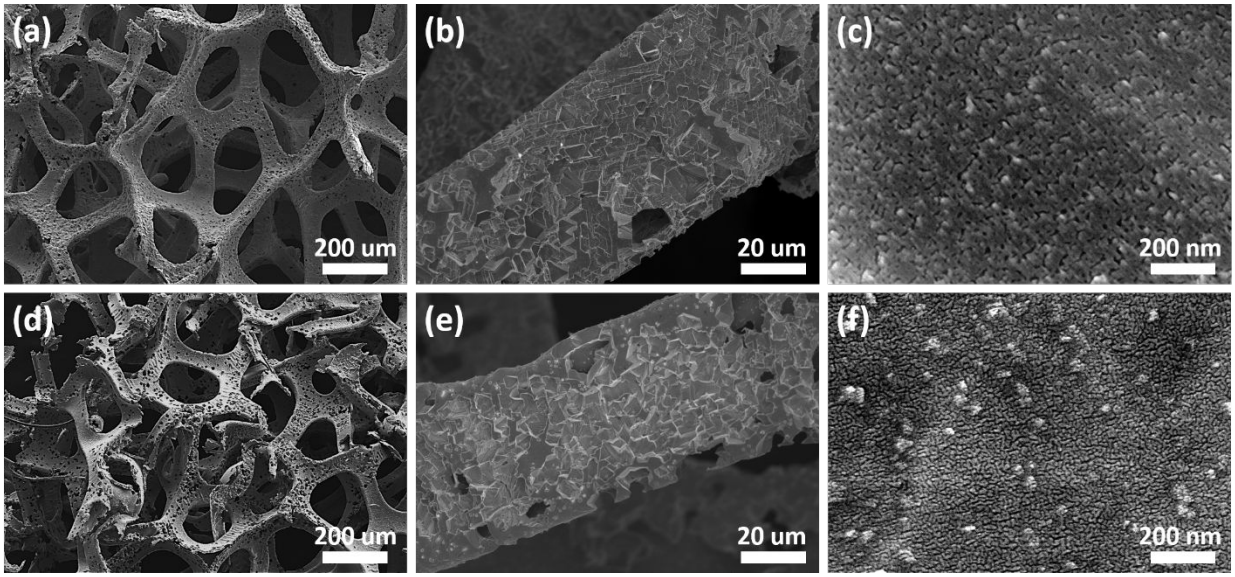

Fig. S14 SEM images of (a), (b), (c) sample 0.14M Fe/A-NF before chronoamperometric stability test, and (d), (e), (f) after chronoamperometric stability test at 500 mA/cm^2 for 24 hrs as cathode.

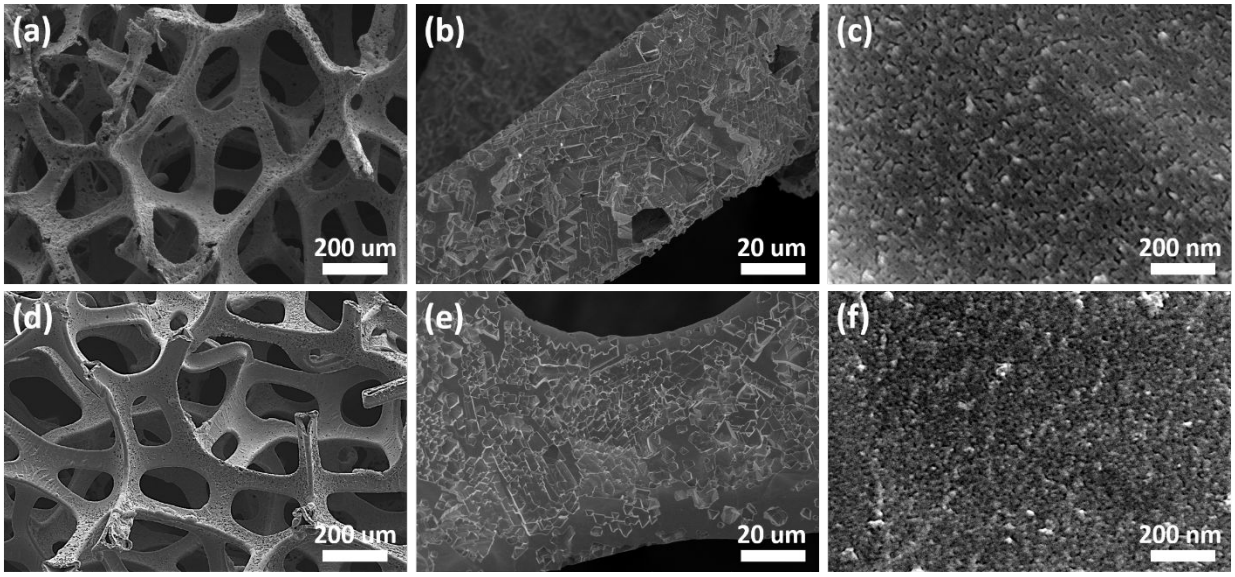

Fig. S15 SEM images of (a), (b), (c) sample 0.14M Fe/A-NF before chronoamperometric stability test, and (d), (e), (f) after chronoamperometric stability test at 500 mA/cm^2 for 24 hrs as anode.

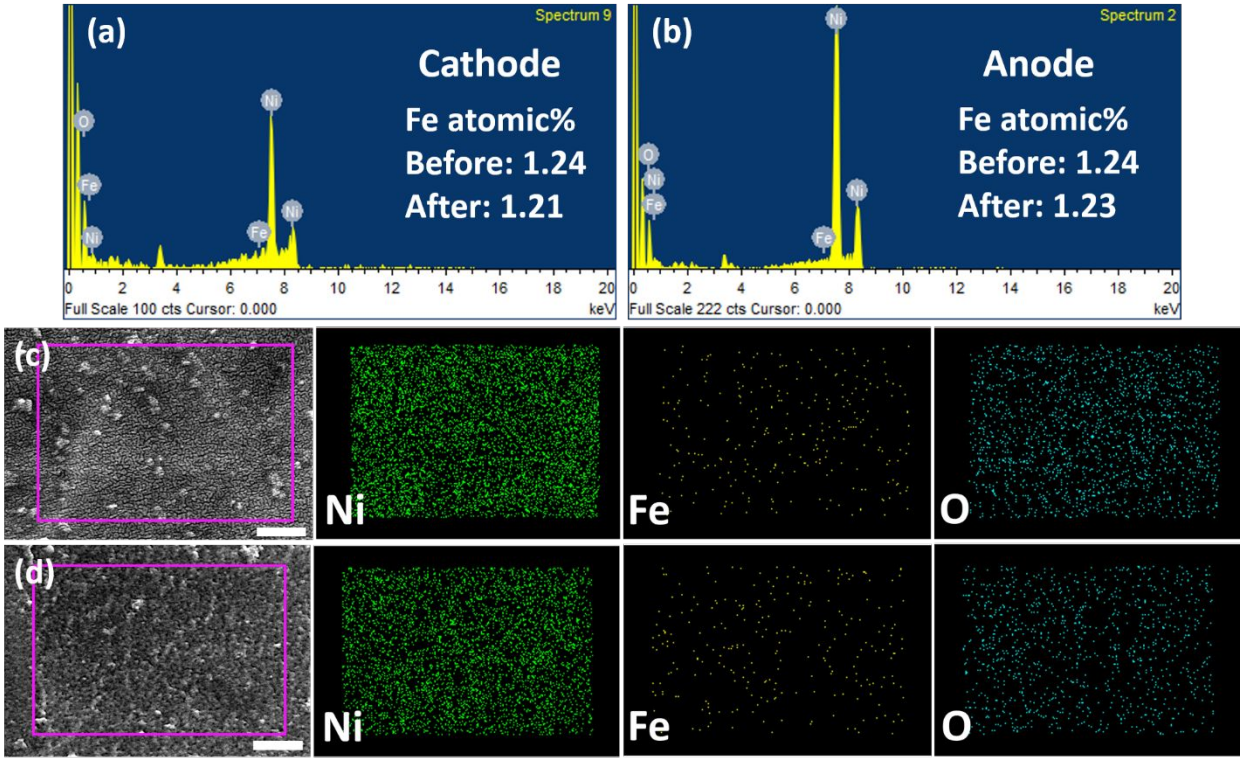

Fig. S16 EDX spectra of sample 0.14M Fe/A-NF after chronoamperometric stability test at 500 mA/cm^2 for 24 hrs: (a) as cathode and (b) as anode. Elemental mapping of sample 0.14M Fe/A-

NF after chronoamperometric stability test at 500 mA/cm^2 for 24 hrs: (c) as cathode and (d) as anode.

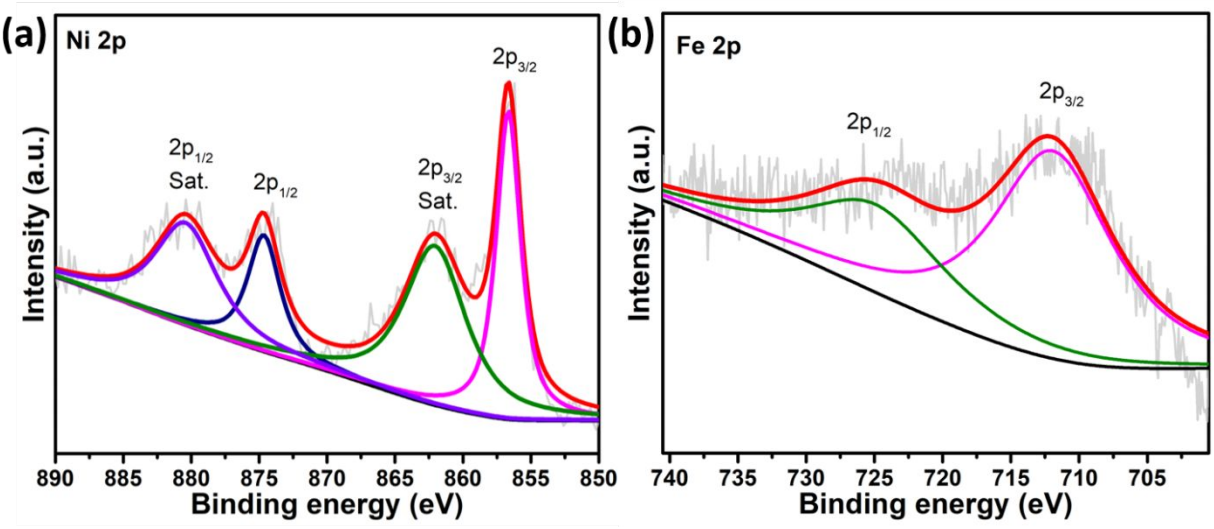

Fig. S17 HRXPS spectrum of sample 0.14M Fe/A-NF after chronoamperometric stability test at 500 mA/cm^2 for 24 hrs as cathode: (a) Ni 2p and (b) Fe 2p.

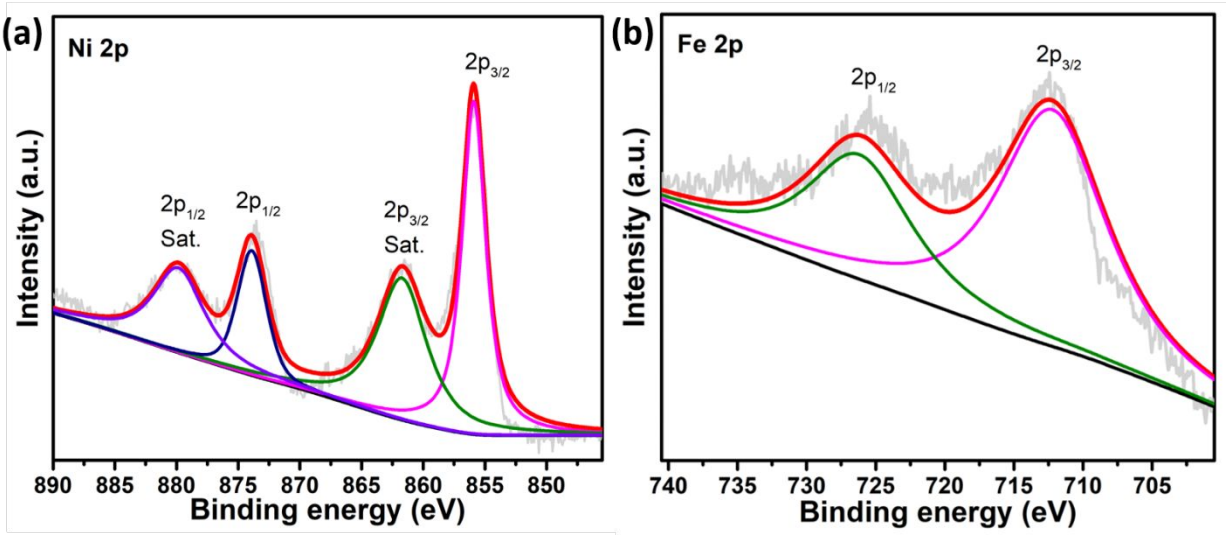

Fig. S18 HRXPS spectrum of sample 0.14M Fe/A-NF after chronoamperometric stability test at 500 mA/cm^2 for 24 hrs as anode: (a) Ni 2p and (b) Fe 2p.

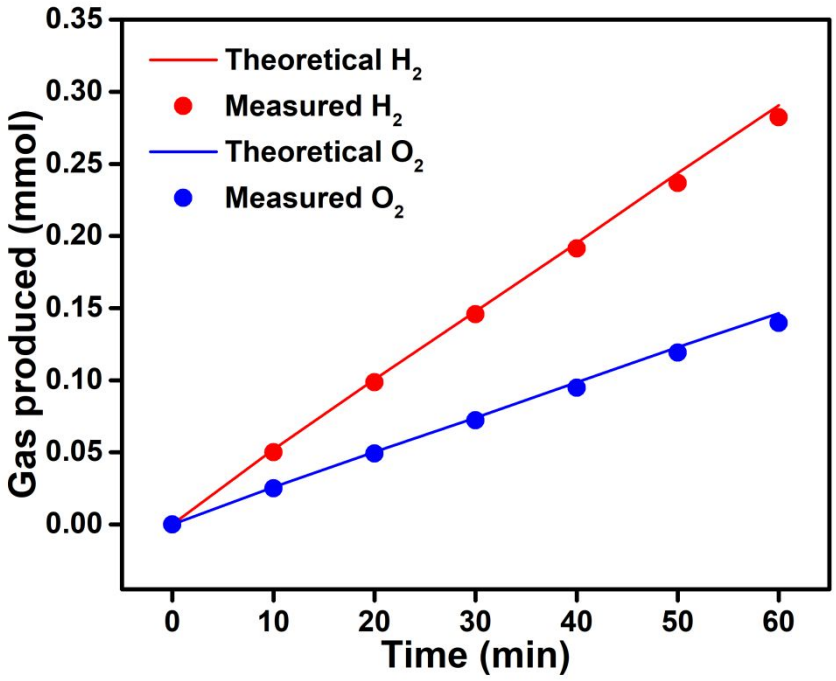

Fig. S19 Experimental and theoretical amounts of H_2 and O_2 production by 0.14M Fe/A-NF//0.14M Fe/A-NF couple for overall water splitting at 80 mA/cm^2.

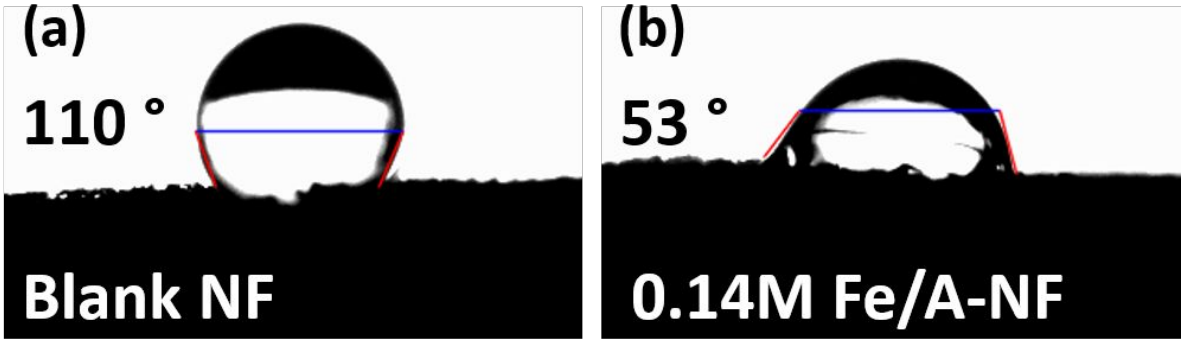

Fig. S20 Static contact angle measurements for (a) blank NF and (b) sample 0.14M Fe/A-NF, showing hydrophilic nature of both samples.

Table S1 OER and overall water splitting performances of NF-based bifunctional electrocatalysts: this work vs. literature.

Catalyst	η (mV) (OER)	Working Potential (V) (Overall water splitting)	Durability test (Overall water splitting)	Ref.
0.14M Fe/A-NF	244 ($50\ mA/cm^2$) 334 ($500\ mA/cm^2$)	1.76 ($50\ mA/cm^2$) 1.99 ($500\ mA/cm^2$)	Chronoamperometry (i-t), 50 & 500 mA/cm^2 @ 24 hrs	**This work**
Co-doped $NiO/NiFe_2O_4$/NF	186 ($10\ mA/cm^2$)	1.58 ($10\ mA/cm^2$)	Chronopotentiometry (v-t), 20 mA/cm^2 @ 20 hrs	1
Fe-doped NiO/NF	206 ($10\ mA/cm^2$)	1.58 ($10\ mA/cm^2$)	Chronopotentiometry (v-t), 20 mA/cm^2 @ 20 hrs	2
NiFe-P/NF	204 ($20\ mA/cm^2$)	1.56 ($10\ mA/cm^2$)	Chronopotentiometry (v-t), 10 mA/cm^2 @ 12 hrs	3
$NiFe/NiCo_2O_4$/NF	310 ($500\ mA/cm^2$) 340 ($1200\ mA/cm^2$)	1.67 ($10\ mA/cm^2$)	Chronopotentiometry (v-t), 20 mA/cm^2 @ 10 hrs	4
NH_2-MIL-88B(Fe_2Ni)/NF	240 ($10\ mA/cm^2$) 335 ($250\ mA/cm^2$) 360 ($500\ mA/cm^2$)	1.56 ($10\ mA/cm^2$) 1.84 ($250\ mA/cm^2$) 1.96 ($500\ mA/cm^2$)	Chronoamperometry (i-t), 250 & 500 mA/cm^2 @ 30 hrs Chronopotentiometry (v-t), 250 & 500mA/cm^2 @ 30 hrs	5
NiFeRu-LDH/NF	225 ($10\ mA/cm^2$)	1.52 ($10\ mA/cm^2$)	Chronopotentiometry (v-t), 10 mA/cm^2 @ 10 hrs	6
NiFe-OH-PO_4/NF	249 ($20\ mA/cm^2$) 280 ($100\ mA/cm^2$)	1.68 ($20\ mA/cm^2$) 1.91 ($100\ mA/cm^2$)	Chronoamperometric (i-t), 20 & 100 mA/cm^2 @ 20 hrs	7
NiFe LDH-NiSe/NF	240 ($100\ mA/cm^2$)	1.53 ($10\ mA/cm^2$) 1.84 ($100\ mA/cm^2$)	Chronoamperometric (i-t), 12 & 114 mA/cm^2 @ 75 hrs	8
Ni-P/NF	357 ($20\ mA/cm^2$)	1.69 ($20\ mA/cm^2$)	Chronoamperometric (i-t), 28 mA/cm^2 @ 20 hrs	9
Co/Fe-doped NiO_xH_y/NF	239 ($10\ mA/cm^2$) 270 ($50\ mA/cm^2$)	1.58 ($10\ mA/cm^2$) 1.72 ($50\ mA/cm^2$)	Chronopotentiometry (v-t), 10 & 50 mA/cm^2 @ 50 hrs	10
N-Ni_3S_2/NF	330 ($100\ mA/cm^2$)	1.48 ($10\ mA/cm^2$) 1.66 ($50\ mA/cm^2$)	Chronoamperometric (i-t), 20 mA/cm^2 @ 8 hrs	11
NiFeMo/NF	238 ($10mA/cm^2$)	1.45 ($10\ mA/cm^2$)	Chronoamperometric (i-t), 20 mA/cm^2 @ 50 hrs	12

Ni,Fe(OOH)/NF	259 (500 mA/cm^2) 289 (1000 mA/cm^2)	1.586 (500 mA/cm^2) 1.657 (1000 mA/cm^2)	Chronopotentiometry (v-t), 30, 500, 1000 & 1500 mA/cm^2 @ 40 hrs	13
FeP/Ni_2P/NF	154 (10 mA/cm^2)	1.42 (10 mA/cm^2) 1.72 (500 mA/cm^2)	Chronopotentiometry (v-t), 30, 100 & 500 mA/cm^2 @ 36 hrs	14

Note that the electrolytes used for all above studies were 1M KOH.

References

(1) Wu, Z. C.; Wang, X.; Huang, J. S.; Gao, F. A Co-doped Ni-Fe mixed oxide mesoporous nanosheet array with low overpotential and high stability towards overall water splitting. *J. Mater. Chem. A* **2018,** *6*, 167-178.

(2) Wu, Z. C.; Zou, Z. X.; Huang, J. S.; Gao, F. Fe-doped NiO mesoporous nanosheets array for highly efficient overall water splitting. *J. Catal.* **2018,** *358*, 243-252.

(3) Xing, J. H.; Li, H.; Cheng, M. M. C.; Geyer, S. M.; Ng, K. Y. S. Electro-synthesis of 3D porous hierarchical Ni-Fe phosphate film/Ni foam as a high-efficiency bifunctional electrocatalyst for overall water splitting. *J. Mater. Chem. A* **2016,** *4*, 13866-13873.

(4) Xiao, C. L.; Li, Y. B.; Lu, X. Y.; Zhao, C. Bifunctional Porous NiFe/$NiCo_2O_4$/Ni Foam Electrodes with Triple Hierarchy and Double Synergies for Efficient Whole Cell Water Splitting. *Adv. Funct. Mater.* **2016,** *26*, 3515-3523.

(5) Senthil Raja, D.; Chuah, X. F.; Lu, S. Y. In Situ Grown Bimetallic MOF-Based Composite as Highly Efficient Bifunctional Electrocatalyst for Overall Water Splitting with Ultrastability at High Current Densities. *Adv. Energy Mater.* **2018**, 1801065.

(6) Chen, G. B.; Wang, T.; Zhang, J.; Liu, P.; Sun, H. J.; Zhuang, X. D.; Chen, M. W.; Feng, X. L. Accelerated Hydrogen Evolution Kinetics on NiFe-Layered Double Hydroxide Electrocatalysts by Tailoring Water Dissociation Active Sites. *Adv. Mater.* **2018,** *30*, 1706279.

(7) Lei, Z. W.; Bai, J. J.; Li, Y. B.; Wang, Z. L.; Zhao, C. Fabrication of Nanoporous Nickel-Iron Hydroxylphosphate Composite as Bifunctional and Reversible Catalyst for Highly Efficient Intermittent Water Splitting. *ACS Appl. Mater. Interfaces* **2017,** *9*, 35837-35846.

(8) Dutta, S.; Indra, A.; Feng, Y.; Song, T.; Paik, U. Self-Supported Nickel Iron Layered Double Hydroxide-Nickel Selenide Electrocatalyst for Superior Water Splitting Activity. *ACS Appl. Mater. Interfaces* **2017,** *9*, 33766-33774.

(9) Xiao, J.; Lv, Q. Y.; Zhang, Y.; Zhang, Z. Y.; Wang, S. One-step synthesis of nickel phosphide nanowire array supported on nickel foam with enhanced electrocatalytic water splitting performance. *RCS Adv.* **2016,** *6*, 107859-107864.

(10) Zhao, Q. H.; Yang, J. L.; Liu, M. Q.; Wang, R.; Zhang, G. X.; Wang, H.; Tang, H. T.; Liu, C. K.; Mei, Z. W.; Chen, H. B.; Pan, F. Tuning Electronic Push/Pull of Ni-Based Hydroxides To Enhance Hydrogen and Oxygen Evolution Reactions for Water Splitting. *ACS Catal.* **2018,** *8*, 5621-5629.

(11) Chen, P.; Zhou, T.; Zhang, M.; Tong, Y.; Zhong, C.; Zhang, N.; Zhang, L.; Wu, C.; Xie, Y. 3D Nitrogen-Anion-Decorated Nickel Sulfides for Highly Efficient Overall Water Splitting. *Adv. Mater.* **2017,** *29*, 1701584.

(12) Qin, F.; Zhao, Z.; Alam, M. K.; Ni, Y.; Robles-Hernandez, F.; Yu, L.; Chen, S.; Ren, Z.; Wang, Z.; Bao, J. Trimetallic NiFeMo for Overall Electrochemical Water Splitting with a Low Cell Voltage. *ACS Energy Lett.* **2018,** *3*, 546-554.

(13) Zhou, H.; Yu, F.; Zhu, Q.; Sun, J.; Qin, F.; Luo, Y.; Bao, J.; Yu, Y.; Chen, S.; Ren, Z. Water splitting by electrolysis at high current density under 1.6 volt. *Energy Environ. Sci.* **2018,** *11*, 2858-2864.

(14) Lu, X. Y.; Zhao, C. A. Electrodeposition of hierarchically structured three-dimensional nickel-iron electrodes for efficient oxygen evolution at high current densities. *Nat. Commun.* **2015,** *6*, 6616.